Reevaluation of the Takano–Oonishi Scheme for Momentum Advection on Bottom Relief in Ocean Models

HIROSHI ISHIZAKI AND TATSUO MOTOI

Meteorological Research Institute, Tsukuba, Japan

(Manuscript received 2 September 1997, in final form 4 December 1998)

ABSTRACT

In the Takano and Oonishi models the finite-difference analog of the nonlinear momentum advection contains the concept of diagonally upward/downward mass and momentum fluxes along the bottom slope, and the generalized Arakawa scheme for the horizontal advection, modified to be fit to arbitrary coastal shape. It has been said to have a good performance, but is not widely used, largely because of its complicated expression.

The purpose of this paper is to reevaluate the Takano–Oonishi scheme for the momentum advection to put it to more practical use by using the redefinition of it in a simple, generalized form and the confirmation of its good performance through a comparison with other schemes.

Based on the definition of mass continuity for a momentum cell (U cell) in terms of that for tracer cells (T cell), the vertical and horizontal mass and momentum fluxes for the U cell are generalized on arbitrary bottom relief in simple forms. Although the grid spacing of the present model is different from that of the Geophysical Fluid Dynamics Laboratory model, applicability of the present scheme to the latter grid spacing is discussed.

Then, the present scheme is tested in an eddy-resolving ocean model and its results are compared with those of a traditional scheme. The present scheme shows good performance in computational efficiency as well as reality of the simulated flow field.

1. Introduction

With advances in supercomputers, the number of numerical experiments and simulations using eddy-resolving ocean models has increased (e.g., Semtner and Chervin 1988, 1992; Böning and Budich 1992; Böning and Herrmann 1994). Based on scale analysis, the nonlinear momentum advection term in these models becomes relatively more important than in coarse models compared to other dominant terms such as the Coriolis force and pressure gradient.

Bryan (1969) proposed a relatively simple momentum advection scheme. In his scheme and its consequent versions of the Geophysical Fluid Dynamics Laboratory (GFDL) model (Cox 1984), the mass continuity for momentum cells (hereafter referred to as U cell) and for tracer (temperature and salinity) cells (hereafter referred to as T cell) are separately calculated from a given set of velocities. The horizontal and vertical mass fluxes advecting horizontal momentum are calculated independently of those for tracers. We call this symbolically ''TC-independent'' U-cell mass continuity. Webb (1995) showed that spurious vertical mass flux for the U cell and its momentum advection appear at near-grid-size features in this code, the largest error magnitude of which increases as the grid size is reduced.

On the other hand, Takano (1978) and Oonishi (1978) developed other schemes in which the mass fluxes for momentum advection are related to those for tracer advection. That is, the U-cell mass continuity is derived from the T-cell mass continuity using a volume-weighted average. This was derived in the process of the generalization of the Arakawa scheme for the vorticity advection term, which formally conserves total square vorticity, to the momentum advection term in the primitive equation system (hereafter referred to as the generalized Arakawa scheme; Arakawa 1966, 1972). We call this type of mass continuity ''TC-dependent'' U-cell mass continuity. We need to use this type of mass continuity when we use the generalized Arakawa scheme. Semtner and Mintz (1977) also used a similar formulation for the U-cell mass continuity. Webb (1995) showed that the errors in the U-cell vertical mass flux appearing in the Cox code were greatly reduced by introducing a TC-dependent U-cell mass continuity equivalent to this. The MOM2 code also uses a similar method (Pacanowski 1995) to avoid decoupling of the two types of W.

Another difference between the GFDL and Takano–Oonishi models is the location of depth definition and coastlines. In the former the ocean domain consists of full T cells, and depth is defined at the center of T cells.

Corresponding author address: Hiroshi Ishizaki, Oceanographic Research Department, Meteorological Research Institute, 1-1 Nagamine, Tsukuba, Ibaraki-ken 305, Japan.

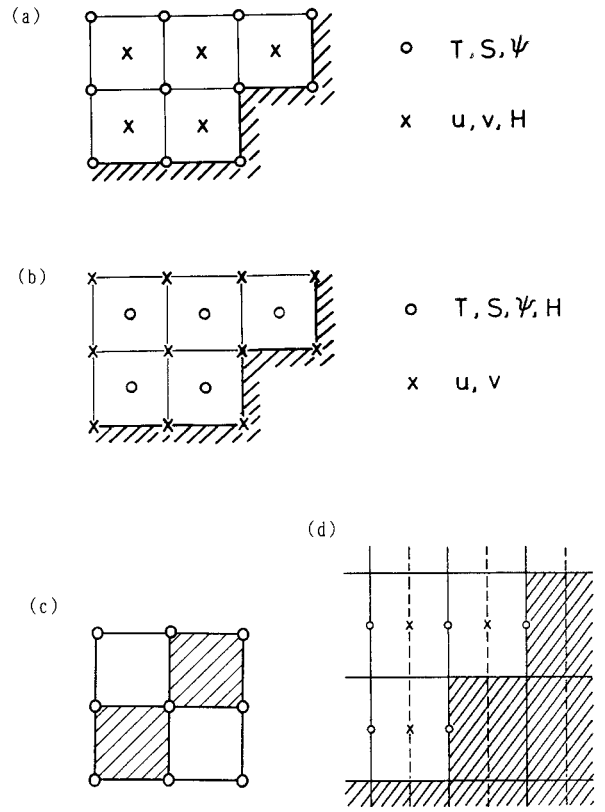

FIG. 1. (a) Horizontal grid spacing for the present model (the TP-coast grid). Tracers (temperature T and salinity S) and barotropic streamfunction Ψ are defined at points marked by (○), and velocity components u and v and depth H are defined at points marked by (×). (b) Horizontal grid spacing for the GFDL model (the UP-coast grid). Depth H is defined at tracer points. Both (a) and (b) are based on Arakawa's B-grid scheme. (c) Mosaic grid pattern. In the present model, the two sea cells are regarded to be connected to each other. (d) Vertical grid spacing of the present model. In all panels, hatched regions designate land cells.

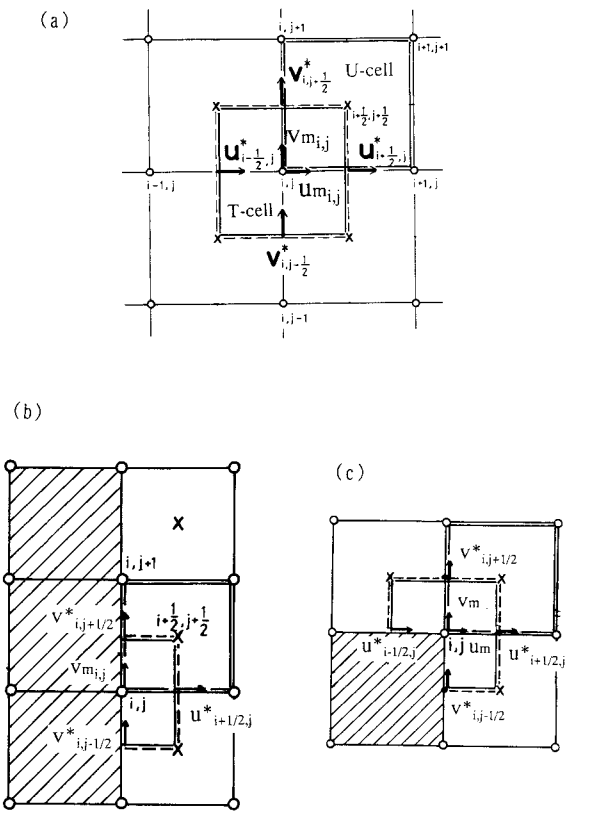

FIG. 2. Definition of locations of mean velocities u^*, v^*, u_m, and v_m: (a) standard case, and (b) and (c) for coastal regions.

Coasts are defined by lines connecting U points (Fig. 1b). Partial U cells appear near topography. In the latter, however, they are reversed; that is, the domain consists of full U cells with depth defined at their centers and coastlines are defined by lines connecting T points (Fig. 1a). Partial T cells are contained. We call the two kinds of grid arrangements simply ''UP-coast'' grid and ''TP-coast'' grid, respectively.

The definition of the mass continuity for a U cell and the grid arrangement are essentially independent events. But the TP-coast grid seems to be natural to the TC-dependent U-cell mass continuity discussed in detail in this paper, and the UP-coast grid seems to be natural to the TC-independent U-cell mass continuity similar to the Cox code, as discussed later in section 5.

As stated in Semtner and Mintz (1977), the TC-independent U-cell mass continuity based on the UP-coast grid and its related momentum advection (the original Cox code) permit a simpler numerical formulation, but they do not guarantee momentum conservation at the side walls, that is, at partial U cells. This is because velocities there are set to be zero to conserve total kinetic energy, in spite of nonzero momentum flux divergence/convergence there. Killworth et al. (1991) modified it so as to conserve momentum at cliffs (i.e., partial cells) by turning the horizontally incoming momentum flux to the vertically outgoing one. In this case, however, the total kinetic energy is not conserved because the advected momentum by the vertically outgoing momentum flux is not the mean of velocities in the adjacent two cells.

In Takano's and Oonishi's schemes, their finite difference forms of mass continuities are essentially identical to each other. For the T-cell mass continuity, vertical mass flux W at the bottom is set to be zero, but W can take a nonzero value at sloping bottom for U cells. This is interpreted as a diagonally upward or downward mass flux along the bottom slope, which naturally emerges in the derivation of the U-cell mass continuity in terms of the T-cell one, on bottom relief. For horizontal momentum advection, both used the generalized Arakawa scheme (Arakawa 1966, 1972). Their standard forms applied to the U cells without any land cells around are the same, but the definitions of advected momentum are somewhat different near a coast or bottom relief. Takano's formula conserves total (or domain-

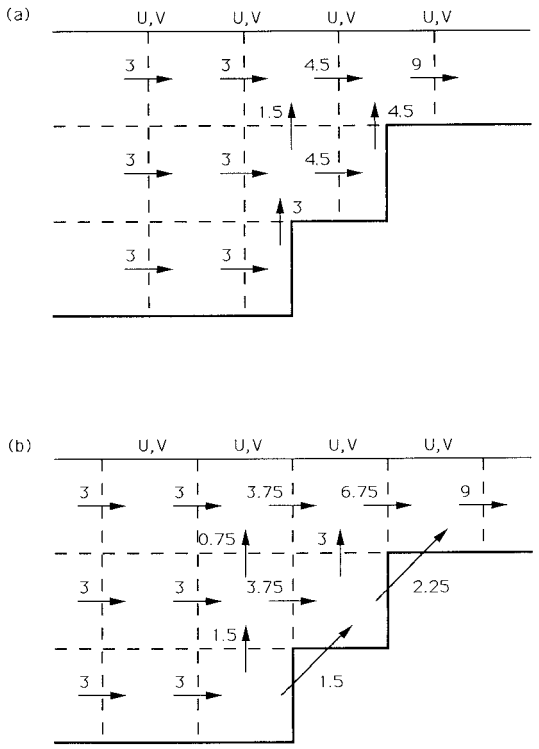

FIG. 3. (a) Two-dimensional mass fluxes for T cells on the stairlike topography. (b) Two-dimensional mass fluxes for U cells on the same topography. These panels are reproduced from Oonishi (1978).

averaged) momentum in the process of advection with arbitrary bottom topography, while Oonishi's formula conserves both total momentum and kinetic energy.

Semtner and Mintz (1977) also developed a model with the TP-coast grid, partial vertical steps, alongslope diagonal flow, and the generalized Arakawa scheme, though the depth variation in their model was only one-dimensional. Their way of treating the topography is more sophisticated than the Takano–Oonishi scheme in the sense that the diagonal flow is explicitly defined within one layer at the bottom as well as at the layer boundaries. We think extension of their method to general geometry may be harder than the Takano–Oonishi scheme.

The purpose of this paper is to reevaluate the Takano–Oonishi scheme for the momentum advection to put it to a more practical use, by the redefinition of it in a simple generalized form, and the confirmation of its good performance through a comparison with other traditional schemes. We logically believe a superiority of these schemes because of three features involved. First, their definition of the U-cell vertical mass flux is, in its standard form, identical to Webb's (1995) new definition of that (i.e., an average of four surrounding T-cell vertical mass fluxes), which prevents decoupling of the two kinds of *W*. Second, they include the generalized Arakawa scheme, which prevents false energy cascade (Arakawa 1972). Finally, they can conserve both total momentum and kinetic energy in the process of advection over arbitrary bottom relief (Takano's scheme can be also rewritten so as to conserve both).

To accomplish our purpose, we first define the U-cell mass continuity as the sum of the contribution from the three-dimensional mass divergence/convergence of four surrounding T cells based on Cartesian coordinates (section 2).

Second, we generalize the definition of the vertical mass flux for U cells and its momentum advection on arbitrary bottom relief in section 3. Both Takano (1978) and Oonishi (1978) insisted on the necessity of introducing diagonally upward/downward mass flux and its momentum advection, but their example involved only stairlike topography; that is, the bottom depth changed in only one direction. We develop this idea to be applicable to cases in which the bottom depth changes arbitrarily.[1] Accurate appreciation of the vertical velocity is important to accurately simulate the horizontal circulation, in particular, in the deep and abyssal seas.

Third, we derive a general formula expressing the horizontal mass and momentum fluxes for U cells near coastlines in terms of those for surrounding T cells in section 4. Its standard form is modified to fit the generalized Arakawa scheme in appendix B. The horizontal mass and momentum fluxes around land cells were given by Takano (1978) and Oonishi (1978) for each shape of coastline. We can express them by a single formula, which we derived.

In section 5 the basic condition for the derivation of the U-cell mass continuity is somewhat relaxed, for the present scheme to fit to usual geophysical coordinates and smoothly varying bottom depths. Applicability of the present scheme to the GFDL-model grid spacing (the UP-coast grid) is also discussed.

Finally, in section 6, we test the present scheme using an eddy-resolving ocean model and compare the results to those obtained by another momentum advection scheme with the widely used TC-independent U-cell mass continuity.

Section 7 is devoted to summary and discussion.

2. Grid arrangement and mass continuity for the standard case

a. Horizontal and vertical grid arrangement

Figure 1a shows the horizontal grid arrangement we use, with coastlines defined by those combining T points (TP-coast grid). Depth is defined at U points; that is, each momentum cell has a constant depth. This is different from the GFDL model's definition, where coastlines are defined by those connecting U points (UP-coast

[1] Later, we found that Takano (1986) treated diagonally upward advection of momentum over two-dimensionally varying topography for situations shown in our Figs. 4 and 5. His definition of advected momentum, however, was different from ours, kinetic energy not being conserved.

grid, Fig. 1b). Both are called Arakawa B-grid spacing. In the mosaic pattern in Fig. 1c we regard the two sea areas as connected. Otherwise, T and S would have to be doubly defined at the central T point.

We take the Cartesian coordinate with fixed increments ΔX and ΔY, and assume, for now, that the vertical grid interval ΔZ takes a fixed value in each layer (Fig. 1d). Relaxation of this condition is discussed later in section 5.

In the following discussion, we use the central difference scheme for all finite differencing so that they are mathematically correct to $O(\Delta^2)$ for equally spaced grids, where Δ is the grid spacing. For unequally spaced grids such as vertical spacing, they are correct to $O(\Delta)$. At the wall, the perpendicular differencing is also correct to $O(\Delta)$.

b. Mass conservation and mass fluxes for tracer advection

The distributions of mean velocities u^* and v^* used for the T-cell mass fluxes U^T and V^T are shown in Fig. 2a. The continuity equation for T cell $(i, j, k + 1/2)$ is expressed by

$$\mathrm{MC}^T_{i,j} \equiv U^T_{i-1/2,j} - U^T_{i+1/2,j} + V^T_{i,j-1/2} - V^T_{i,j+1/2} + W^T_{i,j,k+1} - W^T_{i,j,k} = 0, \tag{1}$$

where

$$U^T_{i+1/2,j} = u^*_{i+1/2,j}\Delta Y\Delta Z, \qquad V^T_{i,j+1/2} = v^*_{i,j+1/2}\Delta X\Delta Z, \tag{2}$$

$$u^*_{i+1/2,j} = \frac{1}{2}(u_{i+1/2,j+1/2} + u_{i+1/2,j-1/2}),$$

$$v^*_{i,j+1/2} = \frac{1}{2}(v_{i+1/2,j+1/2} + v_{i-1/2,j+1/2}), \tag{3}$$

and W^T are vertical mass fluxes for the tracer cell, if there is no coast around the cells (standard definition). The vertical suffix $k + 1/2$ is omitted in the above expressions except for W^T. Index k increases downward. In a region along a coastline (Fig. 2b) the following definitions are taken for the partial T cell (i, j):

$$V^T_{i,j+1/2} = \frac{1}{2}v^*_{i,j+1/2}\Delta X\Delta Z; \qquad V^T_{i,j-1/2} = \frac{1}{2}v^*_{i,j-1/2}\Delta X\Delta Z;$$

$$U^T_{i-1/2,j} = 0, \tag{4}$$

where

$$v^*_{i,j+1/2} = v_{i+1/2,j+1/2}, \qquad v^*_{i,j-1/2} = v_{i+1/2,j-1/2}, \quad \text{and}$$

$$u^*_{i-1/2,j} = 0. \tag{5}$$

For the case of Fig. 2c,

$$U^T_{i-1/2,j} = \frac{1}{2}u^*_{i-1/2,j}\Delta Z\Delta Y;$$

$$V^T_{i,j-1/2} = \frac{1}{2}v^*_{i,j-1/2}\Delta Z\Delta X, \tag{6}$$

where

$$u^*_{i-1/2,j} = u_{i-1/2,j+1/2} \quad \text{and} \quad v^*_{i,j-1/2} = v_{i+1/2,j-1/2}. \tag{7}$$

The boundary conditions for $W^T_{i,j}$ are

$$W^T_{i,j} = 0$$

at the sea surface and at the bottom. (If a free-surface condition is applied, this is only for the bottom.)

c. Mass conservation and mass fluxes for momentum advection

We define mass continuity for U cell $(i + 1/2, j + 1/2)$ (Fig. 2a) from those for surrounding T cells as

$$\mathrm{MC}^U_{i+1/2,j+1/2,k+1/2} \equiv \frac{\mathrm{MC}^T_{i,j,k+1/2}}{N_{i,j,k+1/2}} + \frac{\mathrm{MC}^T_{i+1,j,k+1/2}}{N_{i+1,j,k+1/2}} + \frac{\mathrm{MC}^T_{i,j+1,k+1/2}}{N_{i,j+1,k+1/2}} + \frac{\mathrm{MC}^T_{i+1,j+1,k+1/2}}{N_{i+1,j+1,k+1/2}} = 0, \tag{8}$$

where $N_{i,j,k+1/2}$ is the number of sea cells around the T point (i, j) in layer $k + 1/2$. If T cell (i, j) is a partial cell, $N_{i,j,k+1/2}$ is less than 4. The T-cell mass continuity $\mathrm{MC}^T_{i,j,k+1/2}$ expresses the three-dimensional mass convergence over the cell volume so that $\mathrm{MC}^T_{i,j,k+1/2}/N_{i,j,k+1/2}$ is its part included in U cell $(i + 1/2, j + 1/2)$. Equation (8) means that the U-cell mass convergence consists of the sum of the contributions from the four surrounding T cells, their size proportional to $1/N$. Therefore, in the physical meaning, the U-cell mass continuity is strictly expressed based on the T-cell mass continuity by (8). This equation was not explicit in Takano (1978) nor Oonishi (1978), but is necessary to use the generalized Arakawa scheme.

For the standard case, that is, without any coast and bottom topography around the grid cell concerned, all N in (8) are 4, and (8) is written as

$$\frac{1}{2}(U^U_{i,j} + U^U_{i,j+1}) - \frac{1}{2}(U^U_{i+1,j} + U^U_{i+1,j+1}) + \frac{1}{2}(V^U_{i,j} + V^U_{i+1,j}) - \frac{1}{2}(V^U_{i,j+1} + V^U_{i+1,j+1}) = W^U_{i+1/2,j+1/2,k} - W^U_{i+1/2,j+1/2,k+1}. \tag{9}$$

Here, $U^U_{i,j}$, $V^U_{i,j}$, and $W^U_{i+1/2,j+1/2,k}$ are defined as

$$U^U_{i,j} = u_{m_{i,j}}\Delta Z\Delta Y; \qquad V^U_{i,j} = v_{m_{i,j}}\Delta Z\Delta X,$$

where

$$u_{m_{i,j}} = \frac{1}{2}(u^*_{i+1/2,j} + u^*_{i-1/2,j}),$$

$$v_{m_{i,j}} = \frac{1}{2}(v^*_{i,j+1/2} + v^*_{i,j-1/2}), \tag{10}$$

as shown in Fig. 2a, and

$$W^U_{i+1/2,j+1/2,k} = \frac{1}{4}(W^T_{i,j,k} + W^T_{i+1,j,k} + W^T_{i,j+1,k} + W^T_{i+1,j+1,k}). \tag{11}$$

Further, only for the standard case,

$$U^U_{i,j} = \frac{1}{2}(U^T_{i+1/2,j} + U^T_{i-1/2,j});$$

$$V^U_{i,j} = \frac{1}{2}(V^T_{i,j+1/2} + V^T_{i,j-1/2}). \tag{12}$$

Equation (9) with (11) and (12) gives a formulation of the U-cell mass continuity equivalent to that given by Webb (1995).

Corresponding to the generalized Arakawa scheme [see (26) in section 4], for the standard case, the mass continuity (9) is rewritten as

$$\begin{aligned}
&\frac{2}{3}\left[\frac{1}{2}(U^U_{i,j} + U^U_{i,j+1}) - \frac{1}{2}(U^U_{i+1,j} + U^U_{i+1,j+1}) + \frac{1}{2}(V^U_{i,j} + V^U_{i+1,j}) - \frac{1}{2}(V^U_{i,j+1} + V^U_{i+1,j+1})\right] \\
&\quad + \frac{1}{3}\left[\frac{1}{2}(U^U_{i,j} + V^U_{i,j}) - \frac{1}{2}(U^U_{i+1,j+1} + V^U_{i+1,j+1}) + \frac{1}{2}(U^U_{i,j+1} - V^U_{i,j+1}) - \frac{1}{2}(U^U_{i+1,j} - V^U_{i+1,j})\right] \\
&\quad = W^U_{i+1/2,j+1/2,k} - W^U_{i+1/2,j+1/2,k+1}.
\end{aligned} \tag{13}$$

Here, let us consider the physical meaning of $U^U_{i,j}$ and $V^U_{i,j}$. The left-hand side of (9) means the convergence of the axis-parallel horizontal mass fluxes, and $(1/2)U^U_{i,j}$ and $(1/2)V^U_{i,j}$ are mass fluxes passing through the U-cell walls with a half grid width. In (13), on the other hand, terms such as $(U^U_{i,j} + V^U_{i,j})$ and $(U^U_{i,j+1} - V^U_{i,j+1})$ should be, themselves, regarded as horizontally diagonal mass fluxes, recalling the original Arakawa scheme for the vorticity advection (Arakawa 1966). From (12),

$$\begin{aligned}
U^U_{i,j} + V^U_{i,j} &= \frac{1}{2}(U^T_{i-1/2,j} + V^T_{i,j-1/2}) \\
&\quad + \frac{1}{2}(U^T_{i+1/2,j} + V^T_{i,j+1/2}).
\end{aligned} \tag{12′}$$

If the flow is horizontally nondivergent, mass fluxes are expressed in terms of streamfunction. Then, both $(U^T_{i-1/2,j} + V^T_{i,j-1/2})$ and $(U^T_{i+1/2,j} + V^T_{i+1/2,j})$ in (12′) express net mass flux passing through the diagonal line connecting U points $(i - 1/2, j + 1/2)$ and $(i + 1/2, j - 1/2)$ (see Fig. 2a), and $(U^U_{i,j} + V^U_{i,j})$ is the same. Similarly, $(U^U_{i,j+1} - V^U_{i,j+1})$ is net mass flux passing through the line between U points $(i - 1/2,\ j + 1/2)$ and $(i + 1/2,\ j + 1 + 1/2)$. These fluxes correspond to a square formed by four U points $(i + 1/2,\ j - 1/2)$, $(i - 1/2,\ j + 1/2)$, $(i + 1/2,\ j + 1 + 1/2)$, and $(i + 1 + 1/2,\ j + 1/2)$, which is the double of U cell $(i + 1/2, j + 1/2)$. Thus, $(1/2)(U^U_{i,j} + V^U_{i,j})$, etc., in (13) are diagonal mass fluxes for U cell $(i + 1/2,\ j + 1/2)$.

In the next section, we consider the general definition of the vertical mass flux W^U over bottom relief. The horizontal mass fluxes $(1/2)U^U$ and $(1/2)V^U$ for the cases with coastlines were given by Takano (1978) and Oonishi (1978). They were expressed for each coastal shape. We generalize them to be expressed by single formulas in section 4.

3. Generalization of vertical mass flux and its momentum advection

From (8), the vertical mass flux at the upper surface, level k, of U cell $(i + 1/2,\ j + 1/2,\ k + 1/2)$, $\overline{W}^U_{i+1/2,j+1/2,k}$, is defined by surrounding W^T as

$$\begin{aligned}
\overline{W}^U_{i+1/2,j+1/2,k} &= \frac{W^T_{i,j,k}}{N_{i,j,k+1/2}} + \frac{W^T_{i+1,j,k}}{N_{i+1,j,k+1/2}} + \frac{W^T_{i,j+1,k}}{N_{i,j+1,k+1/2}} \\
&\quad + \frac{W^T_{i+1,j+1,k}}{N_{i+1,j+1,k+1/2}}.
\end{aligned} \tag{14}$$

On the other hand, the vertical mass flux at the bottom surface, level k, of U cell $(i + 1/2,\ j + 1/2,\ k - 1/2)$, $\mathcal{W}^U_{i+1/2,j+1/2,k}$, is defined as

$$\begin{aligned}
\mathcal{W}^U_{i+1/2,j+1/2,k} &= \frac{W^T_{i,j,k}}{N_{i,j,k-1/2}} + \frac{W^T_{i+1,j,k}}{N_{i+1,j,k-1/2}} + \frac{W^T_{i,j+1,k}}{N_{i,j+1,k-1/2}} \\
&\quad + \frac{W^T_{i+1,j+1,k}}{N_{i+1,j+1,k-1/2}}.
\end{aligned} \tag{15}$$

Since W^T are continuous at the boundary of vertically adjacent T cells, $\overline{W}^U$ and $\mathcal{W}^U$ seem to be discontinuous at the boundary when N are vertically different, for example, $N_{i,j,k+1/2} < N_{i,j,k-1/2}$, over the bottom relief. However, this apparent discrepancy can be consistently interpreted by introducing diagonally upward or downward mass fluxes as shown below.

a. One-dimensional variation of bottom depth

Before we go on to general cases with two-dimensionally varying bottom depth, we first consider a case in which the bottom depth varies in one direction like stairs, for simplicity, following Oonishi (1978) (Fig. 3). Assume a barotropic current flows over topography. The U points are just intermediate between T points. Figure 3a shows the mass continuity for T cells. The barotropic

flow comes from the left and barotropy is conserved in the shallow region. The vertical velocity is zero at the bottom and its distribution is also reasonable in the shallow region. Figure 3b shows the mass continuity for U cells, derived from those for adjacent T cells. Except for fluxes just on the bottom slope, each flux is obtained as a mean value of neighboring fluxes for T cells. On the bottom slope alone, we must introduce a flux that flows along the slope to conserve mass continuity. The lowermost U cells at the slope have nonzero vertical flux at the bottom. The barotropy of the flow and the distribution of vertical velocity are thereby kept reasonable for fluxes for U cells.

b. Two-dimensional variation of bottom depth

The diagonally upward/downward mass fluxes introduced in the previous simple case are generalized for flows over bottom topography that varies two-dimensionally (three-dimensional flow). For simplicity, we consider a two-layer case without losing generality. Vertical mass fluxes are defined at the interface. We focus on one of the four terms of W^T/N in (14) and (15) for which the number N in the lower layer is less than that in the upper layer. We show how the upward mass flux W^T is distributed as part of W^U when it passes through the interface. First, we consider three examples of bottom relief, then generalize results for these examples.

1) EXAMPLE 1

Consider a case in which all cells are sea in upper and lower layers except for cell **d** in the lower layer (cell $\mathbf{d}_l$) (Fig. 4). We use suffixes l and u to designate the lower and the upper layers. The central T point and T cell (surrounded by broken lines) are represented by *A.* The vertical mass flux W^T at the interface between cells A_l and A_u can be obtained by the mass continuity for T cells defined by (1)–(7) with appropriate boundary conditions. We assume W^T is upward there. The area of cell A_l (3/4 unit measured by area $\Delta X\Delta Y$) is different from that of cell A_u (1 unit), but mass flux W^T should be continuous at the interface.

Next, we consider how this vertical mass flux for the T cell W^T should be distributed to the mass flux W^U of neighboring U cells represented by **a**, **b**, **c**, and **d.** In the lower layer, W^T is shared by three cells, $\mathbf{a}_l$, $\mathbf{b}_l$, and $\mathbf{c}_l$, so the contribution of W^T to each W^U is $W^T/3$, but in the upper layer it is $W^T/4$ because part of W^T should be also shared by W^U at cell $\mathbf{d}_u$. Here W^U at the bottom of cell $\mathbf{d}_u$ is no longer zero. Therefore, $W^T/4$ of the $W^T/3$ shared by each of the three lower sea cells $\mathbf{a}_l$, $\mathbf{b}_l$, and $\mathbf{c}_l$ is purely vertical, and the remaining $W^T/12$ ($=W^T/3 - W^T/4$) flows to cell $\mathbf{d}_u$ through the interface. Gathering these diagonal fluxes from the lower three cells, the total amount entering cell $\mathbf{d}_u$ ($W^T/12 \times 3$) is certainly $W^T/4$. The advected momentum value should be the mean of those at the starting and ending cells of the flux, if the centered difference scheme is used. This is necessary to conserve total kinetic energy.

2) EXAMPLE 2

Next, consider an example in which only cell $\mathbf{b}_l$ is sea in the lower layer and all four cells are sea in the upper layer (Fig. 5). In the lower layer, W^T is shared only by cell $\mathbf{b}_l$ but, in the upper layer, by all four cells. Therefore, $W^T/4$ of W^T at cell $\mathbf{b}_l$ is carried vertically upward and

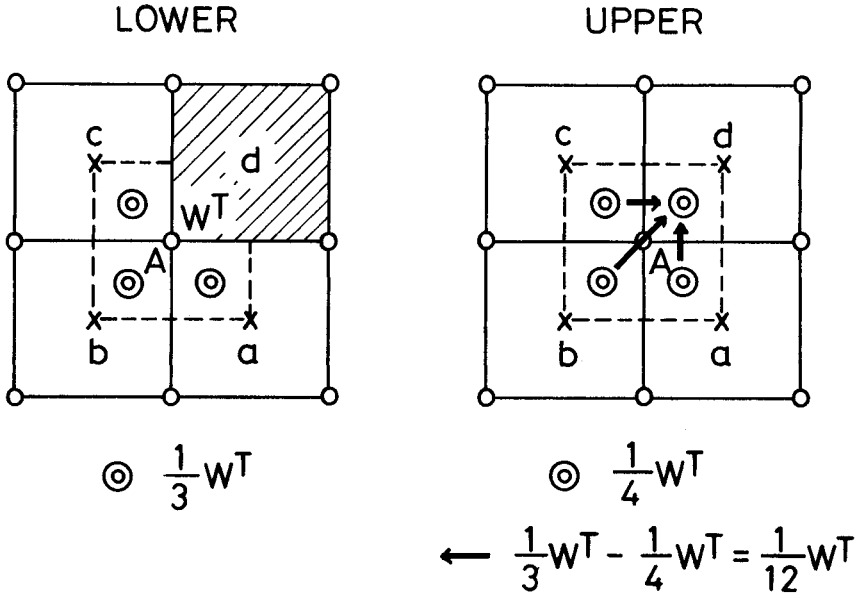

FIG. 4. First example of land–sea patterns, in which all four upper cells are sea, with three sea cells and one land cell in the lower layer.

the remaining $3W^T/4$ is distributed to the other three cells in the upper layer ($\mathbf{a}_u$, $\mathbf{c}_u$, and $\mathbf{d}_u$), each $W^T/4$.

3) EXAMPLE 3

A third example holds that the upper layer also has land area. In this example, cells $\mathbf{c}_l$, $\mathbf{d}_l$, and $\mathbf{d}_u$ are land and others are sea (Fig. 6). In the lower layer, W^T is shared by two cells, $\mathbf{a}_l$ and $\mathbf{b}_l$, while it is shared by three cells, $\mathbf{a}_u$, $\mathbf{b}_u$, and $\mathbf{c}_u$, in the upper layer. Therefore, from each of cells $\mathbf{a}_l$ and $\mathbf{b}_l$, $W^T/3$ of $W^T/2$ goes vertically upward and the remaining $W^T/6$ ($=W^T/2 - W^T/3$) goes diagonally upward to cell $\mathbf{c}_u$ with total amount $W^T/3$ ($=W^T/6 \times 2$).

4) GENERALIZATION

We generalize the relationship between land–sea distribution and vertically and diagonally upward fluxes stated thus far for an arbitrary land–sea distribution. Assume cell $\mathbf{d}_l$ is land but cell $\mathbf{d}_u$ is sea and consider the diagonally upward fluxes coming to cell $\mathbf{d}_u$. We take N_l as the number of sea cells around point A in the lower and N_u the number in the upper layer ($1 \le N_l \le N_u < 4$). Each sea cell in the lower layer carries W^T/N_l, and W^T/N_u of it goes vertically upward. The remaining

$$W^T/N_l - W^T/N_u = W^T(N_u - N_l)/(N_lN_u) \quad (16)$$

should be distributed, as diagonally upward fluxes, to sea cells in the upper layer at which the lower is land. The number of such upper sea cells is $(N_u - N_l)$ including cell $\mathbf{d}_u$. Thus, each diagonally upward flux coming to cell $\mathbf{d}_u$ is

$$W^T(N_u - N_l)/(N_lN_u) \times 1/(N_u - N_l) = W^T/(N_lN_u). \quad (17)$$

The number of such fluxes coming to cell $\mathbf{d}_u$ is N_l, so their total is

$$W^T/(N_lN_u) \times N_l = W^T/N_u. \quad (18)$$

Based on these discussions we understand the difference between (14) and (15).

We regard the name of each cell such as $\mathbf{a}_l$ also as a land–sea index. If we assume that $\mathbf{a}_l = 1$ (0) when cell $\mathbf{a}_l$ is sea (land), then the diagonally upward mass flux and momentum flux coming from cell $\mathbf{a}_l$ to cell $\mathbf{d}_u$ are

$$\mathbf{a}_lW^T/(N_lN_u) \quad \text{and} \quad \mathbf{a}_lW^T(u_{\mathbf{a}_l} + u_{\mathbf{d}_u})/(2N_lN_u), \quad (19)$$

where $u_{\mathbf{a}_l}$ and $u_{\mathbf{d}_u}$ are velocity at cell $\mathbf{a}_l$ and cell $\mathbf{d}_u$, respectively. Purely vertical mass flux and momentum flux from cell $\mathbf{a}_l$ to cell $\mathbf{a}_u$ are

$$\mathbf{a}_lW^T/N_u \quad \text{and} \quad \mathbf{a}_lW^T(u_{\mathbf{a}_l} + u_{\mathbf{a}_u})/(2N_u), \quad (20)$$

respectively, where $u_{\mathbf{a}_u}$ is velocity at cell $\mathbf{a}_u$. Similar formulations apply to cells $\mathbf{b}_l$ and $\mathbf{c}_l$.

Similar calculations for mass and momentum fluxes for W^T at other T points around cell $\mathbf{d}_u$ should be made to complete vertically and diagonally upward momentum advections around cell $\mathbf{d}_u$. When $N_u = N_l$, diagonally upward fluxes need not be considered and only purely vertical fluxes (20) apply.

4. Generalization of horizontal mass flux and its momentum advection

a. Horizontal mass fluxes

Next we consider the generalization of the U-cell horizontal mass fluxes for arbitrary coastal lines, the standard form of which was given by (10) and (11). To do this, we start with the generalization of the T-cell mass continuity (1)–(7). Assuming that $e_{i+1/2,\,j+1/2}$ is a land–sea index (unity for sea and zero for land) for U cell $(i + 1/2,\, j + 1/2)$, the general formulas for $U^T_{i+1/2,\,j}$ and $V^T_{i,j+1/2}$ [(2), (4), and (6)] are given as

$$U^T_{i+1/2,\,j} = \frac{1}{2}(e_{i+1/2,j-1/2} + e_{i+1/2,j+1/2})u^*_{i+1/2,j}\Delta Y\Delta Z$$

and

$$V^T_{i,\,j+1/2} = \frac{1}{2}(e_{i-1/2,\,j+1/2} + e_{i+1/2,\,j+1/2})v^*_{i,\,j+1/2}\Delta X\Delta Z. \quad (21)$$

Substituting them into the mass continuity for T cell (i, j) (1), the horizontal part of the mass continuity for U cell $(i + 1/2, j + 1/2)$ (8), $\mathrm{HMC}^U(i + 1/2, j + 1/2)$, multiplied by its own land–sea signature $e_{i+1/2,\,j+1/2}$, yields

$$\begin{aligned}\mathrm{HMC}^U_{i+1/2,\,j+1/2} = e_{i+1/2,\,j+1/2}\Bigg[&e_{i-1/2,\,j+1/2}\left(\frac{1}{N_{i,j}}U^U_{i,j} + \frac{1}{N_{i,j+1}}U^U_{i,j+1}\right) - e_{i+3/2,\,j+1/2}\left(\frac{1}{N_{i+1,\,j}}U^U_{i+1,\,j} + \frac{1}{N_{i+1,\,j+1}}U^U_{i+1,\,j+1}\right)\\ &+ e_{i+1/2,\,j-1/2}\left(\frac{1}{N_{i,j}}V^U_{i,j} + \frac{1}{N_{i+1,\,j}}V^U_{i+1,\,j}\right) - e_{i+1/2,\,j+3/2}\left(\frac{1}{N_{i,j+1}}V^U_{i,j+1} + \frac{1}{N_{i+1,\,j+1}}V^U_{i+1,\,j+1}\right)\\ &+ e_{i-1/2,\,j-1/2}\frac{1}{N_{i,j}}(U^U_{i,j} + V^U_{i,j}) - e_{i+3/2,\,j+3/2}\frac{1}{N_{i+1,\,j+1}}(U^U_{i+1,\,j+1} + V^U_{i+1,\,j+1})\\ &+ e_{i-1/2,\,j+3/2}\frac{1}{N_{i,j+1}}(U^U_{i,j+1} - V^U_{i,j+1}) - e_{i+3/2,\,j-1/2}\frac{1}{N_{i+1,\,j}}(U^U_{i+1,\,j} - V^U_{i+1,\,j})\Bigg]. \quad (22)\end{aligned}$$

Detailed derivation of (22) is given in appendix A. Assuming mass fluxes M_{E}, M_{N}, M_{NE}, and M_{SE} as follows:

$$
\begin{aligned}
M_{\mathrm{E}_{i,j+1/2}} &= e_{i+1/2,j+1/2}e_{i-1/2,j+1/2}\left(\frac{1}{N_{i,j}}U^U_{i,j} + \frac{1}{N_{i,j+1}}U^U_{i,j+1}\right)\\
M_{\mathrm{N}_{i+1/2,j}} &= e_{i+1/2,j+1/2}e_{i+1/2,j-1/2}\left(\frac{1}{N_{i,j}}V^U_{i,j} + \frac{1}{N_{i+1,j}}V^U_{i+1,j}\right),\\
M_{\mathrm{NE}_{i,j}} &= e_{i+1/2,j+1/2}e_{i-1/2,j-1/2}\frac{1}{N_{i,j}}(U^U_{i,j} + V^U_{i,j}),\\
M_{\mathrm{SE}_{i,j}} &= e_{i-1/2,j+1/2}e_{i+1/2,j-1/2}\frac{1}{N_{i,j}}(U^U_{i,j} - V^U_{i,j}),
\end{aligned}
\tag{23}
$$

then

$$
\begin{aligned}
&\mathrm{HMC}^U_{i+1/2,j+1/2}\\
&\quad = M_{\mathrm{E}_{i,j+1/2}} - M_{\mathrm{E}_{i+1,j+1/2}} + M_{\mathrm{N}_{i+1/2,j}} - M_{\mathrm{N}_{i+1/2,j+1}}\\
&\quad + M_{\mathrm{NE}_{i,j}} - M_{\mathrm{NE}_{i+1,j+1}} + M_{\mathrm{SE}_{i,j+1}} - M_{\mathrm{SE}_{i+1,j}}.
\end{aligned}
\tag{24}
$$

Here, M_{E} and M_{N} are axis-parallel mass fluxes, and M_{NE} and M_{SE} are horizontally diagonal ones (Fig. 7). These formulas of the mass fluxes are essentially identical to those by Takano (1978) and Oonishi (1978), except for the case with $N = 4$.

If we again derive the formula for the standard case from (22) (all of N are 4),

$$
\begin{aligned}
\mathrm{HMC}^U_{i+1/2,j+1/2} = {}& \frac{1}{2}\left[\frac{1}{2}(U^U_{i,j} + U^U_{i,j+1}) - \frac{1}{2}(U^U_{i+1,j} + U^U_{i+1,j+1}) + \frac{1}{2}(V^U_{i,j} + V^U_{i+1,j}) - \frac{1}{2}(V^U_{i,j+1} + V^U_{i+1,j+1})\right]\\
&+ \frac{1}{2}\left[\frac{1}{2}(U^U_{i,j} + V^U_{i,j}) - \frac{1}{2}(U^U_{i+1,j+1} + V^U_{i+1,j+1}) + \frac{1}{2}(U^U_{i,j+1} - V^U_{i,j+1}) - \frac{1}{2}(U^U_{i+1,j} - V^U_{i+1,j})\right].
\end{aligned}
\tag{25}
$$

This expression is different from the horizontal mass flux convergence for the generalized Arakawa scheme (13). Both express that the horizontal mass flux convergence is a mean of those of the axis-parallel mass fluxes and of the diagonal ones. But the weight of the averaging is 2/3:1/3 for the generalized Arakawa scheme, while it is 1/2:1/2 for the present one. We will discuss this point next.

b. Horizontal momentum advection

We could use the generalized formulas of the U-cell horizontal mass fluxes (23) as they are, for those of horizontal momentum fluxes. However, its standard form (25) is different from that derived from the generalized Arakawa scheme (13). For the standard case, we have the freedom to choose one of various weights of averaging between the convergence of the axis-parallel mass fluxes and the convergence of the horizontally diagonal ones. For example, if we assume α and β are the weights for the former and the latter, respectively, we can choose any combination of α and β as long as $\alpha + \beta = 1$. For (25), $\alpha = \beta = 1/2$. There is a combination $\alpha = 1$ and $\beta = 0$, which yields the left-hand side of (9) and corresponds to Webb's (1995) formulation. Among them, we choose the generalized Arakawa scheme, that is, $\alpha = 2/3$, $\beta = 1/3$, for the standard case, because our purpose is to reevaluate Takano's (1978) and Oonishi's (1978) scheme. Following Takano (1978), convergence of the horizontal momentum advection for U cell $(i + 1/2, j + 1/2)$, $\mathrm{CAD}_{i+1/2,j+1/2}(u)$ is written as

$$
\begin{aligned}
\mathrm{CAD}_{i+1/2,j+1/2}(u) = {}& \frac{2}{3}\left[\frac{1}{2}(u_{i-1/2,j+1/2} + u_{i+1/2,j+1/2})\frac{1}{2}(U^U_{i,j} + U^U_{i,j+1}) - \frac{1}{2}(u_{i+1/2,j+1/2} + u_{i+3/2,j+1/2})\frac{1}{2}(U^U_{i+1,j} + U^U_{i+1,j+1})\right.\\
&\left. + \frac{1}{2}(u_{i+1/2,j-1/2} + u_{i+1/2,j+1/2})\frac{1}{2}(V^U_{i,j} + V^U_{i+1,j}) - \frac{1}{2}(u_{i+1/2,j+1/2} + u_{i+1/2,j+3/2})\frac{1}{2}(V^U_{i,j+1} + V^U_{i+1,j+1})\right]\\
&+ \frac{1}{3}\left[\frac{1}{2}(u_{i+1/2,j+1/2} + u_{i-1/2,j-1/2})\frac{1}{2}(U^U_{i,j} + V^U_{i,j}) - \frac{1}{2}(u_{i+1/2,j+1/2} + u_{i+3/2,j+3/2})\frac{1}{2}(U^U_{i+1,j+1} + V^U_{i+1,j+1})\right.\\
&\left. + \frac{1}{2}(u_{i+1/2,j+1/2} + u_{i-1/2,j+3/2})\frac{1}{2}(U^U_{i,j+1} - V^U_{i,j+1}) - \frac{1}{2}(u_{i+1/2,j+1/2} + u_{i+3/2,j-1/2})\frac{1}{2}(U^U_{i+1,j} - V^U_{i+1,j})\right].
\end{aligned}
\tag{26}
$$

Except for the standard case, of course, we must use the mass fluxes (23) and related momentum fluxes. The merging of the generalized Arakawa scheme for the standard case into them is made in appendix B. The resultant momentum fluxes F_{E}, F_{N}, F_{NE}, and F_{SE} are given as

$$\begin{aligned}
F_{E_{i,j+1/2}}(u) &= \frac{1}{2}(u_{i-1/2,j+1/2} + u_{i+1/2,j+1/2})M_{E_{i,j+1/2}},\\
F_{N_{i+1/2,j}}(u) &= \frac{1}{2}(u_{i+1/2,j-1/2} + u_{i+1/2,j+1/2})M_{N_{i+1/2,j}},\\
F_{NE_{i,j}}(u) &= \frac{1}{2}(u_{i+1/2,j+1/2} + u_{i-1/2,j-1/2})M_{NE_{i,j}},\\
F_{SE_{i,j}}(u) &= \frac{1}{2}(u_{i-1/2,j+1/2} + u_{i+1/2,j-1/2})M_{SE_{i,j}}, \qquad (27)
\end{aligned}$$

where the mass fluxes M_{E}, M_{N}, M_{NE}, and M_{SE} are defined as

$$\begin{aligned}
M_{E_{i,j+1/2}} &= \frac{1}{6}(C_{XN_{i,j}}U^U_{i,j} + C_{XS_{i,j+1}}U^U_{i,j+1}),\\
M_{N_{i+1/2,j}} &= \frac{1}{6}(C_{YE_{i,j}}V^U_{i,j} + C_{YW_{i+1,j}}V^U_{i+1,j}),\\
M_{NE_{i,j}} &= \frac{1}{6}C_{NE_{i,j}}(U^U_{i,j} + V^U_{i,j}),\\
M_{SE_{i,j}} &= \frac{1}{6}C_{SE_{i,j}}(U^U_{i,j} - V^U_{i,j}), \qquad (28)
\end{aligned}$$

and

$$\begin{aligned}
C_{XN_{i,j}} &= e_{i+1/2,j+1/2}e_{i-1/2,j+1/2}(e_{i+1/2,j-1/2}e_{i-1/2,j-1/2}\\
&\qquad - e_{i+1/2,j-1/2} - e_{i-1/2,j-1/2} + 3),\\
C_{XS_{i,j}} &= e_{i+1/2,j-1/2}e_{i-1/2,j-1/2}(e_{i+1/2,j+1/2}e_{i-1/2,j+1/2}\\
&\qquad - e_{i+1/2,j+1/2} - e_{i-1/2,j+1/2} + 3),\\
C_{YE_{i,j}} &= e_{i+1/2,j+1/2}e_{i+1/2,j-1/2}(e_{i-1/2,j+1/2}e_{i-1/2,j-1/2}\\
&\qquad - e_{i-1/2,j+1/2} - e_{i-1/2,j-1/2} + 3),\\
C_{YW_{i,j}} &= e_{i-1/2,j+1/2}e_{i-1/2,j-1/2}(e_{i+1/2,j+1/2}e_{i+1/2,j-1/2}\\
&\qquad - e_{i+1/2,j+1/2} - e_{i+1/2,j-1/2} + 3),\\
C_{NE_{i,j}} &= e_{i+1/2,j+1/2}e_{i-1/2,j-1/2}(3 - e_{i-1/2,j+1/2} - e_{i+1/2,j-1/2}),
\end{aligned}$$

and

$$C_{SE_{i,j}} = e_{i-1/2,j+1/2}e_{i+1/2,j-1/2}(3 - e_{i+1/2,j+1/2} - e_{i-1/2,j-1/2}). \qquad (29)$$

Finally, convergence of the horizontal momentum fluxes is written as

$$\begin{aligned}
&\mathrm{CAD}_{i+1/2,j+1/2}(u)\\
&\quad = F_{E_{i,j+1/2}}(u) - F_{E_{i+1,j+1/2}}(u) + F_{N_{i+1/2,j}}(u)\\
&\qquad - F_{N_{i+1/2,j+1}}(u) + F_{NE_{i,j}}(u) - F_{NE_{i+1,j+1}}(u)\\
&\qquad + F_{SE_{i,j+1}}(u) - F_{SE_{i+1,j}}(u). \qquad (30)
\end{aligned}$$

5. Relaxation of conditions

Here, we relax some conditions assumed in the derivation of the U-cell mass continuity (8) for practical use.

a. Relaxation on the grid sizes

The U-cell mass continuity (8) was derived under the assumption that each MC^T expresses the three-dimensional mass convergence over the T-cell volume and that MC^T/N is its part included in the central U cell. This was achieved in the Cartesian coordinate with fixed increment of ΔX and ΔY. Most of large-scale ocean models, however, consist of grid cells surrounded horizontally by latitude circles and meridian lines. In such cases, the zonal grid interval ΔX and the horizontal cell area have a meridional dependence through the factor of the cosine of latitude. Therefore, strictly speaking, MC^T/N no longer represents part of MC^T included in the central U-cell, that is, the physical concept of (8) is slightly violated. But we must take (8) as it is for the generalized formulas of mass and momentum fluxes so far discussed to hold in these cases. There is no other choice for mathematical expression. In the definitions of V^T (2) and V^U (10), ΔX must be replaced by $\Delta X \cos\theta$, where θ is latitude. For vertical grid interval ΔZ, we have assumed that it takes a fixed value for each layer. As pointed out by Ishizaki (1994), however, if ΔZ is fixed, a gentle bottom slope cannot be suitably expressed if its decline is much smaller than the ratio of the vertical-to-horizontal grid interval. That is, there are wide flat bottoms and cliffs here and there with height ΔZ. In these regions, vertical velocity is concentrated at the cliffs, resulting in relatively strong fictitious horizontal currents there.

We can avoid this by permitting ΔZ in the lowermost layer at each horizontal point to be variable, that is, permitting ΔZ to take any value less than the fixed one on the bottom relief. (Of couse, the vertical CFL condition must be satisfied.) In this case, the horizontal velocity components u and v in the definition of u^* and v^* (3) must be multiplied by r if the U cell is in contact with the bottom, where

$$r_{i+1/2,j+1/2,k+1/2} = \Delta Z^B_{i+1/2,j+1/2,k+1/2}/\Delta Z_{k+1/2}$$

is the ratio of the variable bottom thickness ΔZ^{B} and the nominal thickness ΔZ of the $k + 1/2$th layer. The volume element for the U cell is $\Delta V = \Delta X \Delta V \Delta Z^{\mathrm{B}}$. In this case the physical concept of (8) is also violated, but we need (8) for the mathematically consistent expression by means of finite differencing.

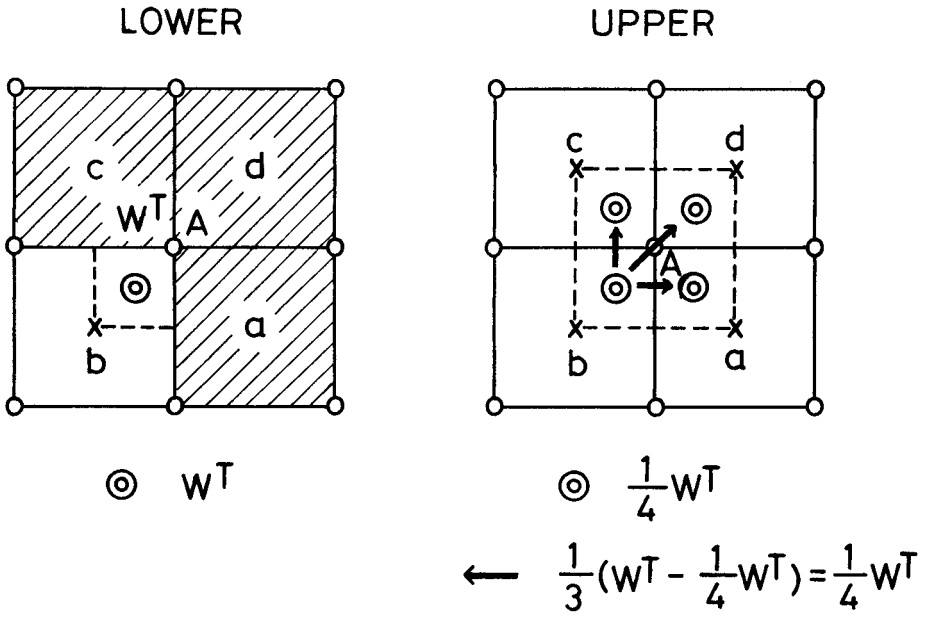

FIG. 5. Second example of land–sea patterns, in which all four upper cells are sea, with one sea cell and three land cells in the lower layer.

b. Application of the present scheme to the UP-coast grid

The difference between the TP-coast grid used here and the UP-coast grid used in the GFDL model originates from the difference in the definition of the partial cells shown with vertical hatching in Figs. 8a,b. In the UP-coast grid they are regarded as partial U cells, while they are regarded as a part of landmass in the TP-coast grid. As discussed in the introduction, as long as momentum advection is concerned, the existence of the partial U cell causes the violation of the conservation of total momentum and/or kinetic energy through the use of the TC-independent U-cell mass continuity. They absorb or emit momentum and/or kinetic energy, in spite of usual zero velocity there. These inconveniences are avoided by preventing the mass and momentum fluxes to enter the partial U cells, that is, by restricting exchanges of these fluxes only between the full U cells.

Assume a set of velocity given on the UP-coast grid. Then, fill up the partial U cells to make the TP-coast grid. The horizontal T-cell mass fluxes on the former grid are identical to those on the latter grid because of zero velocity at the wall in the former, though T-cell volume changes along the wall (partial T cells) in the latter. This means that the vertical T-cell mass fluxes W^T are also identical in both grid systems. Then, only assuming the U-cell land–sea index to be zero also for the partial U cells, the vertical and horizontal mass and momentum fluxes, so far discussed, can be applied to the UP-coast grid. A difference occurs in the tracer convergence because of the difference in volume at partial T cells, though the tracer fluxes are identical on both grids for a given set of variables.

On the other hand, the TC-independent U-cell mass continuity can be formulated on the TP-coast grid, assuming the partial land U cells along the wall absorb or emit mass, momentum, and energy just as the partial U-cells on the UP-coast grid do. We use this formulation for comparison of the scheme performances in the next section.

6. Test of the scheme

Here we test our scheme and compare the results with those by other schemes, using an eddy-resolving model. For the comparison, we coded an equivalent of the original Cox code based on the TP-coast grid, that is, the traditional TC-independent U-cell mass continuity and related momentum fluxes. As discussed before, we can do this assuming that half of the land U-cell adjacent to the coastline (Figs. 8a,b) is effectively a partial sea cell, which absorbs and/or emits mass and momentum fluxes horizontally across the coastal face and vertically across the bottom of the lowest full U cell. In this code, hereafter referred to as the equivalent Cox code (EC code), momentum is not conserved near the topography, though the total kinetic energy is conserved. Diagonally upward/downward momentum advection is not included.

An eddy-resolving regional ocean model has been developed by H. Ishizaki and G. Yamanaka (unpublished manuscript) for the entire North Pacific Ocean with the present scheme for the momentum advection terms. The rigid-lid approximation is used in the model. The domain is 100°E~75°W and 15°S~65°N, with the horizontal resolution ¼° (EW) × ⅙° (NS). The number

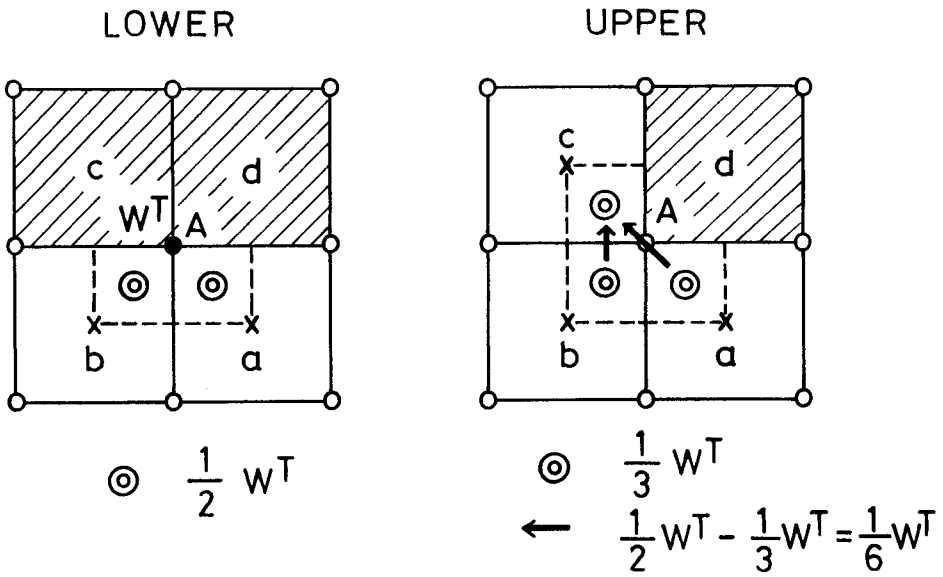

FIG. 6. Third example of land–sea patterns, in which one of the upper cells is land, with two land and two sea cells in the lower layer.

of the vertical levels is 44, with 250-m resolution below 2000 m and finer and variable resolution above the level. The model already has been run for several years from the state of rest with a simple vertical stratification. The monthly mean temperature and salinity data by Levitus (1982) and the monthly mean wind stress data by Hellerman and Rosenstein (1983) have been used as the external forcings. Initially, a large value of the coefficients of biharmonic diffusivity and viscosity 5×10^{18} $cm^4\ s^{-1}$ was used. Then, it has been gradually relaxed to smaller values to fully develop the mesoscale eddies, finally, 1×10^{17} $cm^4\ s^{-1}$ for diffusivity and 3×10^{17} $cm^4\ s^{-1}$ for viscosity. In addition, an effective biharmonic diffusion works, because the QUICK (Quadratic Upstream Interpolation for Convective Kinematics)

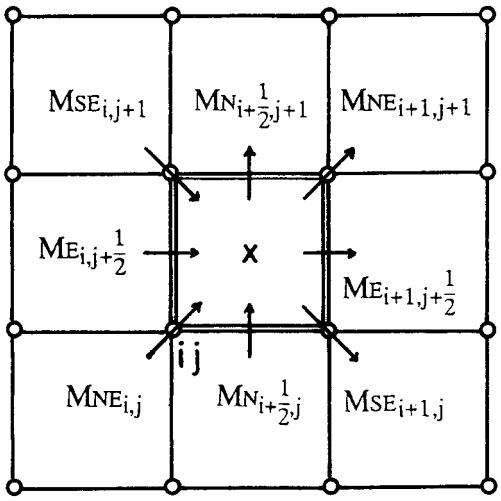

FIG. 7. Distribution of mass fluxes for U cell ($i + 1/2$, $j + 1/2$).

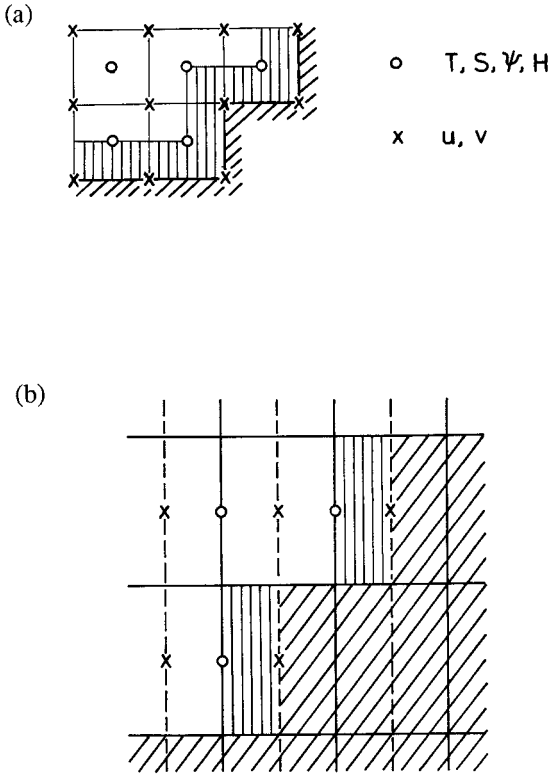

FIG. 8. (a) Horizontal and (b) vertical grid alignment of the GFDL model grid spacing. The vertically hatched regions in both panels mean partial U cells.

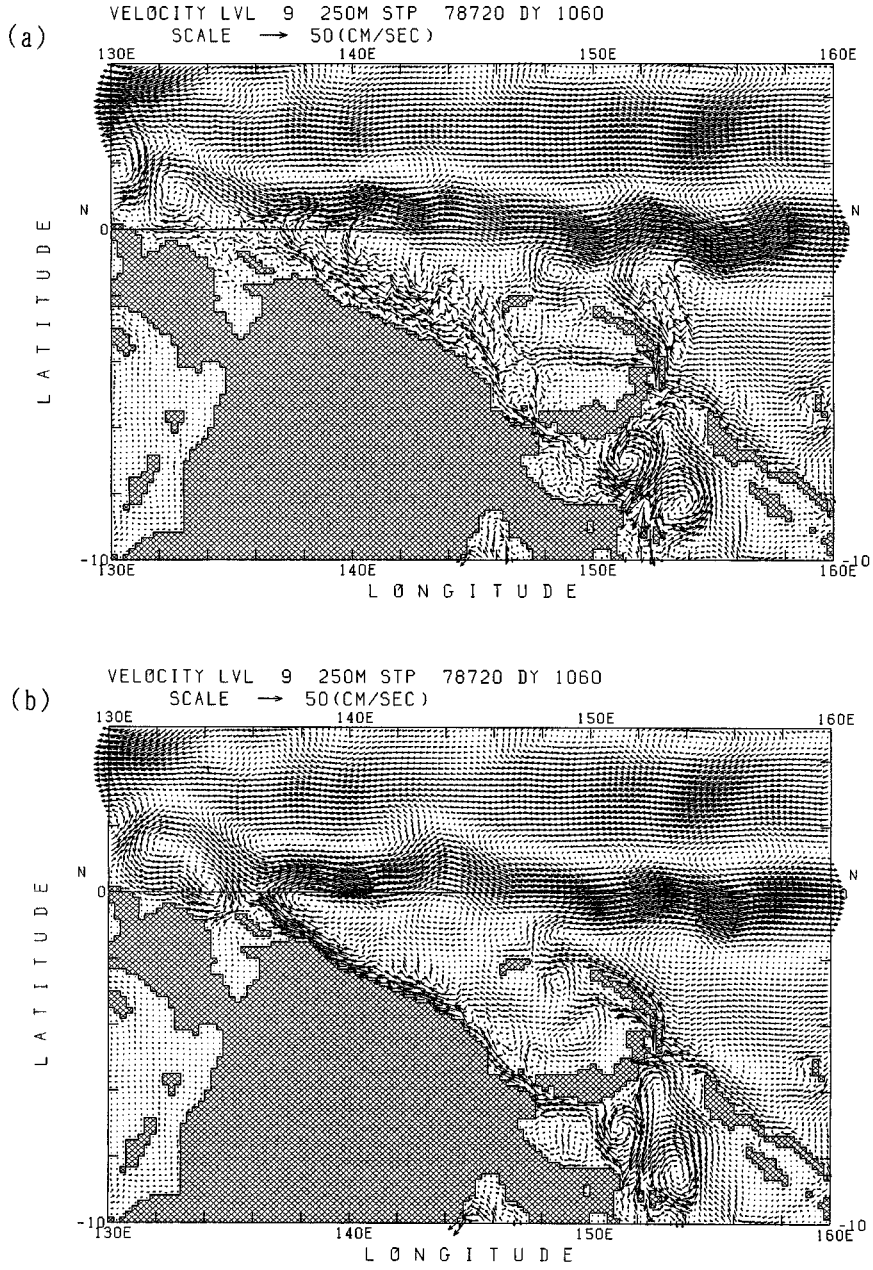

FIG. 9. Velocity at 250 m at day 1060 north of New Guinea for (a) the EC-code run and for (b) the standard run.

scheme is adopted for the tracer advection terms following Holland et al. (1998). The coefficient of the diffusivity is the cube of the grid interval multiplied by local velocity, so it may be greater than the aforementioned values of diffusivity in strong flow regions. We call this the standard experiment or the standard run. The time interval of the integration is constant at 30 min for all runs.

We made two additional runs by means of the EC code, starting from days 1020 and 1500 of the standard experiment. Other conditions were the same as those of the standard experiment. In the former (the first EC-code run) a 40-day integration was made with 1×10^{18} $cm^4\ s^{-1}$ both for diffusivity and viscosity. In the latter (the second EC-code run) the integration duration was 30 days, with the final values of diffusivity (1×10^{17} $cm^4\ s^{-1}$) and viscosity (3×10^{17} $cm^4\ s^{-1}$).

Figure 9 shows the result of the first EC-code run (day 1060) with the corresponding standard run. The most prominent difference in the velocity field at 250 m appears along the northern coast of New Guinea, where the EC-code run indicates a noisy pattern with

grid-scale disturbances (Fig. 9a), while the standard run shows rectified flows (Fig. 9b). The noisy pattern does not appear in the barotropic flow and stratification is most intensive around 300 m in this region. Therefore, the disturbances may be caused by the decoupling of W^U from W^T, as discussed by Webb (1995). It is also suggested that topography influences their existence because the disturbed regions are distributed along the coastlines.

The result of the second EC-code run (day 1530) is shown in Fig. 10 for the region of the Kuroshio south of Japan. This is the region with strongest flows, and the nonlinear momentum advection may be largest there. In this case the EC code requires a shorter time interval less than or equal to 20 min, while the standard run is still stable with a 30-min interval. This EC-code run was made with a 15-min interval. In spite of the shorter time interval, the resultant flow field of the EC-code run (Fig. 10a) is noisier than that of the standard run (Fig. 10b) on both sides of the Kuroshio. Figure 11

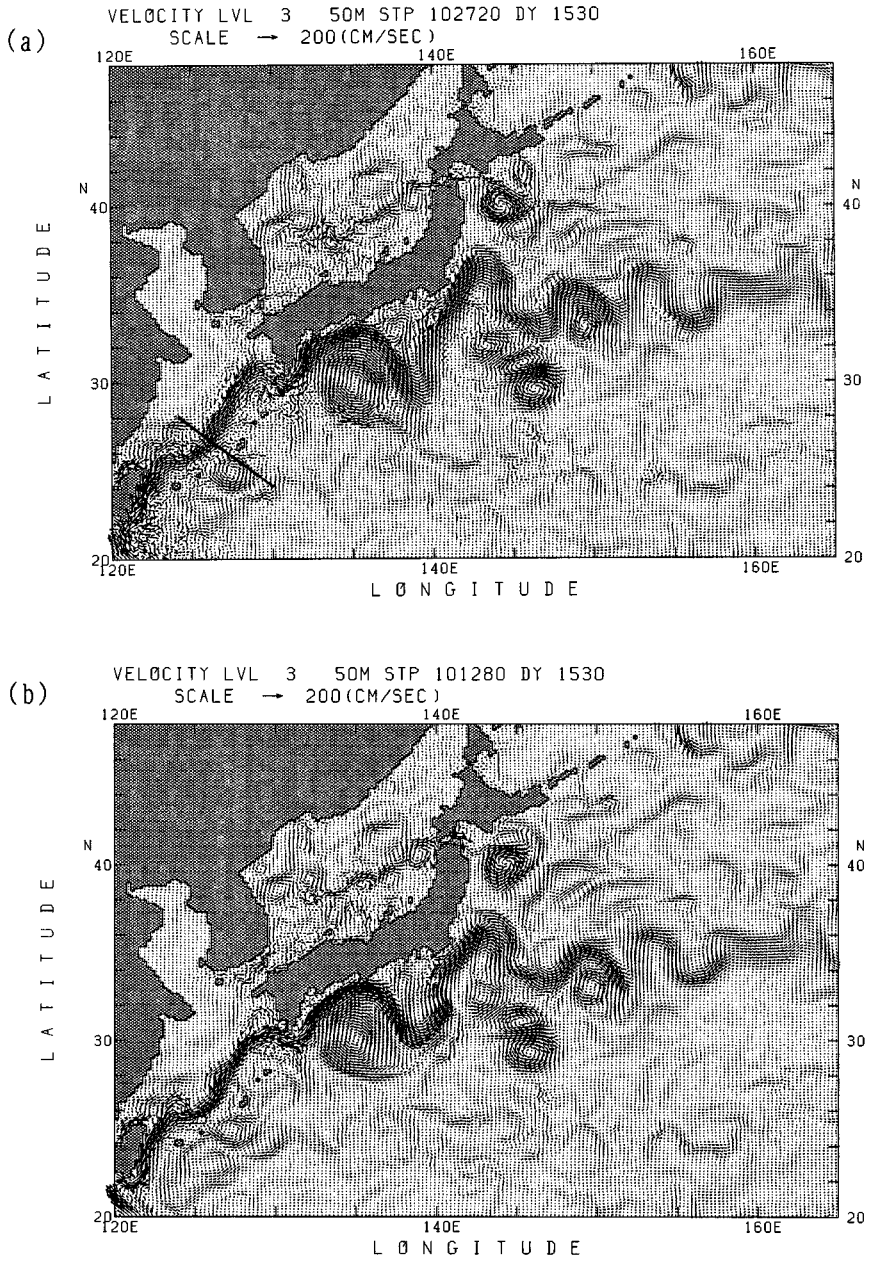

FIG. 10. Velocity at 50 m at day 1530 for regions of the Kuroshio south of Japan for (a) the EC-code run and for (b) the standard run. The line in the east China Sea shown in (a) indicates the section for Fig. 11.

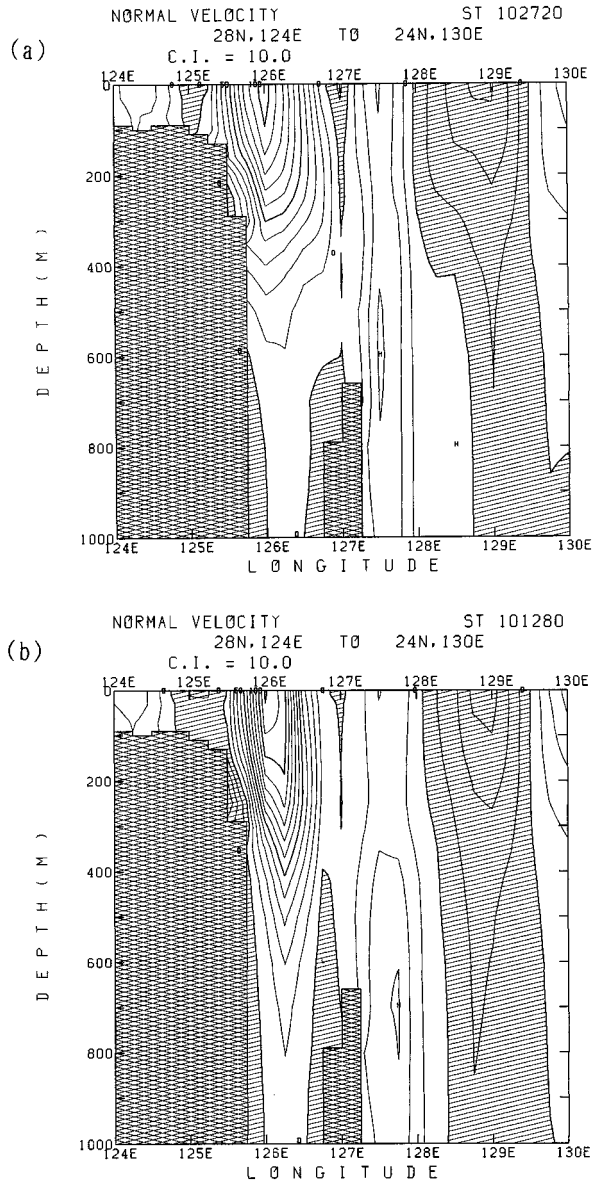

FIG. 11. Vertical section of northeastward velocity along the line shown in Fig. 10a. (a) EC-code run and (b) standard run. Contour interval is 10 cm s^{-1}. The southwestward flow is hatched.

shows the vertical section along the line shown in Fig. 10a of the northeastward flow of the Kuroshio along the shelf break in the east China Sea. It indicates that the core of the Kuroshio is stronger by about 20 cm s^{-1} and is confined to a narrower width in the standard run (Fig.11b) than in the EC-code run (Fig. 11a). The core reaches to deeper levels also in the standard run than in the EC-code run. These features of the standard run indicate evidence of the superiority of the present momentum advection scheme to the EC code, because a noisy scheme may flatten the core and dissipate near-bottom flows.

The domain-averaged kinetic energy of the EC-code run at day 1530 (23.9 ergs) is less than that of the standard run (26.1 ergs) by 8%. This is also related to the noisy feature of the former, because the false cascade of energy to smaller scales leads to its efficient dissipation by the highly scale-selective biharmonic viscosity operator.

From the practical point of view, the standard run requires longer time for one time step computation than the EC-code run does by about 3%, but it is sufficiently compensated by the possibility of taking a longer time step. Computational efficiency is achieved by the present scheme.

7. Summary and discussion

The purpose of this paper is to reevaluate the Takano–Oonishi scheme for momentum advection to put it to more practical use, by redefinition of it in a simple, generalized form and the confirmation of its good performance through a comparison with other traditional scheme. To do this, we first defined the U-cell mass convergence as the sum of the contribution from the three-dimensional mass convergence of four surrounding T cells.

Second, we generalize the expression of vertical mass flux for U cells and its momentum advection on arbitrary bottom relief based on the concept of diagonally upward/downward mass flux along the bottom slope. It was examined how the vertical mass flux for a tracer cell was redefined as the vertical and diagonally upward/downward mass fluxes for surrounding momentum cells on bottom relief.

Third, we derived a general formula of the horizontal mass and momentum fluxes for U cells near coastlines by means of those for surrounding T cells. Its standard form is modified to fit the generalized Arakawa scheme.

Fourth, the basic physical concept in the derivation of the U-cell mass continuity was somewhat relaxed, for the present scheme to fit to usual geographical coordinates and smoothly varying bottom depths. Applicability of the present scheme to the GFDL grid spacing (the UP-coast grid) was also discussed.

Finally, we tested the present scheme using an eddy-resolving ocean model and compared the results to those obtained by another momentum advection scheme with the traditional TC-independent U-cell mass continuity. In general, the present scheme showed better performance compared to the latter in computational efficiency as well as in the realistic simulation of the flow field. Thus, the present scheme was verified for practical application.

The flux forms of the diagonally upward/downward and the vertical momentum fluxes, (19) and (20), and the flux convergence form of the horizontal momentum advection, (27), assures the conservation of total momentum. On the other hand, two conditions are required for mean kinetic energy to be conserved (e.g., Bryan 1969): first, the mass conservation is satisfied for each

U cell; second, the advected velocity is defined as a simple mean of velocities at two adjacent U cells at which the mass flux transport starts and ends. The second condition must be satisfied even for the horizontally and vertically diagonal mass fluxes. The present formulation completely satisfies the two conditions and therefore conserves mean kinetic energy.

For a two-dimensional flow, Arakawa (1966) constructed a Jacobian form that formally conserves the total square vorticity (enstrophy) as well as total kinetic energy. This scheme, the Arakawa scheme, prevents spurious energy cascade. Its generalized form applied to the primitive equation system on the B-grid spacing (27), however, formally conserves not square vorticity but similar quadratic quantities of spatial derivatives of velocity such as $(\partial v/\partial x)^2$ and $(\partial u/\partial y)^2$ in its standard form, for a horizontally nondivergent flow (Arakawa 1972). This also prevents a spurious energy cascade (Arakawa 1972). Although the conservation of these quantities is not formally ensured when topography is included, the test results discussed in section 6 clearly indicate a reduction of the spurious energy cascade to smaller scales by the use of the present scheme with the generalized Arakawa scheme.

Acknowledgments. The authors thank Drs M. Endoh, M. Kamachi, Y. Kitamura, T. Uji, and G. Yamanaka for very helpful discussion and comments. The authors also express their gratitude to the reviewers for their critical and constructive comments and suggestions. This study was funded by the Meteorological Research Institute.

APPENDIX A

Derivation of the Horizontal Part of the U-Cell Mass Continuity with Coastlines

Substituting the generalized formula of T-cell mass fluxes U^T and V^T (21) into the mass continuity for T cell (i, j) (1), the X component of the mass continuity for U cell $(i + 1/2, j + 1/2)$ (8), $\mathrm{XMC}^U(i + 1/2, j + 1/2)$, multiplied by its own land–sea signature $e_{i+1/2,j+1/2}$, is expressed as

$$
\begin{aligned}
\mathrm{XMC}^U_{i+1/2,j+1/2} &= e_{i+1/2,j+1/2}\frac{\Delta Y}{2}\Delta Z \\
&\quad\times\left\{\frac{1}{N_{i,j}}[(e_{i-1/2,j-1/2}+e_{i-1/2,j+1/2})u^*_{i-1/2,j}-(e_{i+1/2,j-1/2}+e_{i+1/2,j+1/2})u^*_{i+1/2,j}]\right. \\
&\qquad+\frac{1}{N_{i+1,j}}[(e_{i+1/2,j-1/2}+e_{i+1/2,j+1/2})u^*_{i+1/2,j}-(e_{i+3/2,j-1/2}+e_{i+3/2,j+1/2})u^*_{i+3/2,j}] \\
&\qquad+\frac{1}{N_{i,j+1}}[(e_{i-1/2,j+1/2}+e_{i-1/2,j+3/2})u^*_{i-1/2,j+1}-(e_{i+1/2,j+1/2}+e_{i+1/2,j+3/2})u^*_{i+1/2,j+1}] \\
&\qquad\left.+\frac{1}{N_{i+1,j+1}}[(e_{i+1/2,j+1/2}+e_{i+1/2,j+3/2})u^*_{i+1/2,j+1}-(e_{i+3/2,j+1/2}+e_{i+3/2,j+3/2})u^*_{i+3/2,j+1}]\right\} \\
&= e_{i+1/2,j+1/2}\frac{\Delta Y}{2}\Delta Z \\
&\quad\times\left\{\left[\frac{1}{N_{i,j}}(e_{i-1/2,j-1/2}+e_{i-1/2,j+1/2})u^*_{i-1/2,j}+\left(-\frac{1}{N_{i,j}}+\frac{1}{N_{i+1,j}}\right)(e_{i+1/2,j-1/2}+e_{i+1/2,j+1/2})u^*_{i+1/2,j}\right.\right. \\
&\qquad\left.-\frac{1}{N_{i+1,j}}(e_{i+3/2,j-1/2}+e_{i+3/2,j+1/2})u^*_{i+3/2,j}\right] \\
&\qquad+\left[\frac{1}{N_{i,j+1}}(e_{i-1/2,j+1/2}+e_{i-1/2,j+3/2})u^*_{i-1/2,j+1}+\left(-\frac{1}{N_{i,j+1}}+\frac{1}{N_{i+1,j+1}}\right)(e_{i+1/2,j+1/2}+e_{i+1/2,j+3/2})u^*_{i+1/2,j+1}\right. \\
&\qquad\left.\left.-\frac{1}{N_{i+1,j+1}}(e_{i+3/2,j+1/2}+e_{i+3/2,j+3/2})u^*_{i+3/2,j+1}\right]\right\}.
\end{aligned}
$$

Here, recalling $N_{i,j} = e_{i-1/2,j-1/2} + e_{i+1/2,j-1/2} + e_{i-1/2,j+1/2} + e_{i+1/2,j+1/2}$, etc.,

$$\left(-\frac{1}{N_{i,j}} + \frac{1}{N_{i+1,j}}\right)(e_{i+1/2,j-1/2} + e_{i+1/2,j+1/2}) = \frac{1}{N_{i,j}}(e_{i-1/2,j-1/2} + e_{i-1/2,j+1/2}) - \frac{1}{N_{i+1,j}}(e_{i+3/2,j-1/2} + e_{i+3/2,j+1/2}) \quad \text{(A1)}$$

and

$$\left(-\frac{1}{N_{i,j+1}} + \frac{1}{N_{i+1,j+1}}\right)(e_{i+1/2,j+1/2} + e_{i+1/2,j+3/2}) = \frac{1}{N_{i,j+1}}(e_{i-1/2,j+1/2} + e_{i-1/2,j+3/2}) - \frac{1}{N_{i+1,j+1}}(e_{i+3/2,j+1/2} + e_{i+3/2,j+3/2}). \quad \text{(A2)}$$

Thus, based on (10),

$$\begin{aligned}\mathrm{XMC}^U_{i+1/2,j+1/2} = e_{i+1/2,j+1/2}\frac{\Delta Y}{2}\Delta Z\Bigg\{&\Bigg[\frac{1}{N_{i,j}}(e_{i-1/2,j-1/2} + e_{i-1/2,j+1/2})(u^*_{i-1/2,j} + u^*_{i+1/2,j}) \\ &- \frac{1}{N_{i+1,j}}(e_{i+3/2,j-1/2} + e_{i+3/2,j+1/2})(u^*_{i+1/2,j} + u^*_{i+3/2,j})\Bigg] \\ &+ \Bigg[\frac{1}{N_{i,j+1}}(e_{i-1/2,j+1/2} + e_{i-1/2,j+3/2})(u^*_{i-1/2,j+1} + u^*_{i+1/2,j+1}) \\ &- \frac{1}{N_{i+1,j+1}}(e_{i+3/2,j+1/2} + e_{i+3/2,j+3/2})(u^*_{i+1/2,j+1} + u^*_{i+3/2,j+1})\Bigg]\Bigg\} \\ = e_{i+1/2,j+1/2}\Bigg[&e_{i-1/2,j+1/2}\left(\frac{1}{N_{i,j}}U^U_{i,j} + \frac{1}{N_{i,j+1}}U^U_{i,j+1}\right) - e_{i+3/2,j+1/2}\left(\frac{1}{N_{i+1,j}}U^U_{i+1,j} + \frac{1}{N_{i+1,j+1}}U^U_{i+1,j+1}\right) + e_{i-1/2,j-1/2}\frac{1}{N_{i,j}}U^U_{i,j} \\ &- e_{i+3/2,j+3/2}\frac{1}{N_{i+1,j+1}}U^U_{i+1,j+1} + e_{i-1/2,j+3/2}\frac{1}{N_{i,j+1}}U^U_{i,j+1} - e_{i+3/2,j-1/2}\frac{1}{N_{i+1,j}}U^U_{i+1,j}\Bigg]. \quad \text{(A3)}\end{aligned}$$

Adding the Y component to (A3) leads to (22) in the text.

APPENDIX B

Merging of the Generalized Arakawa Scheme into the General Form of the Horizontal Momentum Convergence

To merge the generalized Arakawa scheme for the standard case into the general form of the horizontal mass flux expressed by (23) and related momentum flux, let us examine the axis-parallel and the horizontally diagonal mass flux associated with $U^U_{i,j}$

Look at, for example, the right panel of Fig. 4, where letters **a**, **b**, **c**, and **d** designate the land–sea index and names of the U cells. We assume the central T point is (i, j) and that cell **d** $(i + 1/2, j + 1/2)$ is sea (**d** = 1). We analyze the two kinds of mass fluxes associated with $U^U_{i,j}$ under different combinations of **a**, **b**, and **c**. These are shown in Table B1. The number of combinations of **a**, **b**, and **c** is eight (2^3) and the first column in Table

TABLE B1. Definition of a land–sea index, the coefficient identifying each case (column A), the coefficient of $U^U_{i,j}$ in the axis-parallel mass flux (column B), the coefficient of $U^U_{i,j}$ in the horizontally diagonal mass flux (column C), for eight combinations of indices **a**, **b**, and **c** in Fig. 4. The cell **d** is assumed to be sea, and the momentum advection by means of $U^U_{i,j}$ into/from the cell **d** is generalized.

Case	Land–sea index				B	C
					Coefficient of $U^U_{i,j}$ (axis-parallel)	Coefficient of $U^U_{i,j}$ (horizontally diagonal)
n	**a**	**b**	**c**	A	+	×
1	1	1	1	**abc**	1/3	1/6
2	1	1	0	**ab**(1 − **c**)	0	1/3
3	1	0	1	**a**(1 − **b**)**c**	1/3	0
4	0	1	1	(1 − **a**)**bc**	1/3	1/3
5	1	0	0	—	0	0
6	0	1	0	(1 − **a**)**b**(1 − **c**)	0	1/2
7	0	0	1	(1 − **a**)(1 − **b**)**c**	1/2	0
8	0	0	0	—	0	0

B1 shows such combinations. The second column (A) corresponds to a coefficient, which is unity for its own combination and is zero for all other combinations. The third column (B) shows the coefficient of $U^U_{i,j}$ in the axis-parallel mass flux of the U-cell mass continuity (13) or (22). The fourth (C) indicates the coefficient of $U^U_{i,j}$ in the horizontally diagonal mass flux of (13) or (22).

The mass continuity formula for the generalized Arakawa scheme (13) is applied for the case with $N = 4$ (case 1 in Table B1), in which the value is 1/3 for B and 1/6 for C [both would be 1/4, if (22) were taken]. For all other cases, (22) is used. This merging does not violate any of mass, momentum, and kinetic energy conservations

The generalized coefficient of $U^U_{i,j}$ in the axis-parallel mass flux (c_1) is obtained by summing up the product of A and B over the eight cases. Similarly, that in the horizontally diagonal mass flux (c_2) is obtained by the summation of the product of A and C. That is,

$$c_1 = \sum_{n=1}^{8} \mathrm{A}_n\mathrm{B}_n = \frac{1}{6}\mathbf{c}(\mathbf{ab} - \mathbf{a} - \mathbf{b} + 3)$$

and

$$c_2 = \sum_{n=1}^{8} \mathrm{A}_n\mathrm{C}_n = \frac{1}{6}\mathbf{b}(3 - \mathbf{a} - \mathbf{c}). \qquad \text{(B1)}$$

Then, the axis-parallel and the horizontally diagonal flux of momentum (u) related with $U^U_{i,j}$, multiplied by the land–sea signature **d**, are

$$\frac{\mathbf{d}}{2}(u_{\mathbf{c}} + u_{\mathbf{d}})c_1U^U_{i,j} = \frac{1}{2}(u_{\mathbf{c}} + u_{\mathbf{d}})\frac{1}{6}\mathbf{cd}(\mathbf{ab} - \mathbf{a} - \mathbf{b} + 3)U^U_{i,j}$$

and

$$\frac{\mathbf{d}}{2}(u_{\mathbf{b}} + u_{\mathbf{d}})c_2U^U_{i,j} = \frac{1}{2}(u_{\mathbf{b}} + u_{\mathbf{d}})\frac{1}{6}\mathbf{bd}(3 - \mathbf{a} - \mathbf{c})U^U_{i,j}, \qquad \text{(B2)}$$

respectively. These give a definition of mass and momentum fluxes identical to that by Oonishi (1978).

REFERENCES

Arakawa, A., 1966: Computational design for long-term numerical integration of the equation of fluid motion: Two-dimensional incompressible flow. Part I. *J. Comput. Phys.,* **1,** 119–143.

——, 1972: Design of the UCLA General Circulation Model. Numerical Simulation Weather and Climate, Tech. Rep. No. 7, Dept. of Meteorology, University of California, Los Angeles, 116 pp.

Böning, C. W., and R. G. Budich, 1992: Eddy dynamics in a primitive equation model: Sensitivity to horizontal resolution and friction. *J. Phys. Oceanogr.,* **22,** 361–381.

——, and P. Herrmann, 1994: Annual cycle of poleward transport in the ocean: Results from high-resolution modeling of the North and equatorial Atlantic. *J. Phys. Oceanogr.,* **24,** 91–107.

Bryan, K., 1969: A numerical method for the study of the circulation of the world ocean. *J. Comput. Phys.,* **4,** 347–376.

Cox, M. D., 1984: A primitive equation, 3-dimensional model of the ocean. GFDL Ocean Group Tech. Rep. 1, Geophysical Fluid Dynamics Laboratory/NOAA, Princeton, NJ, 143 pp.

Holland, R. W., J. C. Chow, and F. O. Bryan, 1998: Application of a third-order upwind scheme in the NCAR ocean model. *J. Climate,* **11,** 1487–1493.

Hellerman, S., and M. Rosenstein, 1983: Normal monthly wind stress over the world ocean with error estimates. *J. Phys. Oceanogr.,***13,** 1093–1104.

Ishizaki, H., 1994: A simulation of the abyssal circulation in the North Pacific Ocean. Part II: Theoretical rationale. *J. Phys. Oceanogr.,* **24,** 1941–1954.

Killworth, P. D., D. Staniforth, D. J. Webb, and S. M. Paterson, 1991: The development of a free-surface Bryan–Cox–Semtner ocean model. *J. Phys. Oceanogr.,* **21,** 1333–1348.

Levitus, S., 1982: *Climatological Atlas of the World Ocean.* NOAA Prof. Paper 13, U.S. Government Printing Office, 173 pp.

Oonishi, Y., 1978: Method of numerical studies: Marginal seas (in Japanese). *Oceanography as Environmental Science,* S. Horibe, Ed., Tokyo University Press, 246–271.

Pacanowski, R. C., 1995: MOM2 documentation, users guide and reference manual. GFDL Ocean Group Tech. Rep. 3, Geophysical Fluid Dynamics Laboratory/NOAA, Princeton, NJ 232 pp.

Semtner, A. J., Jr., and Y. Mintz, 1977: Numerical simulation of the Gulf Stream and mid-ocean eddies. *J. Phys. Oceanogr.,* **7,** 208–230.

——, and R. M. Chervin, 1988: A simulation of the global ocean circulation with resolved eddies. *J. Geophys. Res.,* **93,** 15 502–15 522.

——, and ——, 1992: Ocean general circulation from a global eddy-resolving model. *J. Geophys. Res.,* **97,** 5493–5550.

Takano, K., 1978: Influences of ridges on deep and bottom flows (in Japanese). *Oceanography as Environmental Science,* S. Horibe, Ed., Tokyo University Press, Tokyo, 27–44.

——, 1986: Structure of numerical model. Report on the deep water motion at a proposed area for ocean dumping of radioactive wastes (in Japanese). Radioactive Waste Management Center, Minato Ward, Tokyo, 191–222.

Webb, D. J., 1995: The vertical advection of momentum in Bryan–Cox–Semtner ocean general circulation models. *J. Phys. Oceanogr.,* **25,** 3186–3195.